Applied Catalysis B: Environmental 127 (2012) 167–174

Contents lists available at SciVerse ScienceDirect

Applied Catalysis B: Environmental

journal homepage: www.elsevier.com/locate/apcatb

Transformation and reduction of androgenic activity of 17α-methyltestosterone in Fe_3O_4/MWCNTs–H_2O_2 system

Xiao-bin Hu[a,b], Yue-hua Deng[a], Zhan-qi Gao[a], Ben-zhi Liu[a], Cheng Sun[a,*]

[a] State Key Laboratory of Pollution Control and Resource Reuse, School of the Environment, Nanjing University, Nanjing 210046, PR China
[b] School of Life Science, Huzhou Teachers College, Huzhou 313000, PR China

ARTICLE INFO

Article history:
Received 17 April 2012
Received in revised form 15 July 2012
Accepted 17 August 2012
Available online 29 August 2012

Keywords:
Fe_3O_4/MWCNTs nanocomposites
Heterogeneous Fenton
17α-Methyltestosterone
Degradation mechanism
Androgenic activity

ABSTRACT

A heterogeneous Fenton catalyst, multiwalled carbon nanotubes (MWCNTs)–supported Fe_3O_4 nanoparticles, Fe_3O_4/MWCNTs was evaluated through the adsorption and degradation of a trace steroidal endocrine disrupting compound (EDC) 17α-methyltestosterone (MT) in water and in the presence of H_2O_2, respectively. The androgenic activity of the treated water was investigated during the catalytic reactions by human androgen ELISA test. The degradation mechanism of MT by Fe_3O_4/MWCNTs catalysis was discussed on the basis of GC–MS analysis of the intermediates and the theoretical calculation of frontier electron densities and bond dissociation enthalpies of C—H and O—H of MT molecule. Competitive oxidation could help to understand that the adsorption of trace MT onto the catalyst was favorable to MT degradation by •OH, which was confirmed by electron spin resonance spin-trapping technique. The results showed that Fe_3O_4/MWCNTs–H_2O_2 system could not only degrade MT but also remove its androgenic activity. The novel catalyst would be of potential application in water treatment for removing natural and synthetic hydrophobic trace pollutants.

1. Introduction

Nowadays, advanced oxidation processes (AOPs) are becoming important technologies for water treatment [1–3]. Fenton method, which mainly uses hydroxyl radical (•OH) as oxidant in the presence of H_2O_2 and catalyst, is the most intensively studied AOP [4–6]. Compared to the homogeneous Fenton, heterogeneous Fenton with wider working pH range and less iron sludge have been attracting more and more attention.

In recent years, different iron hydroxides and iron oxides as heterogeneous catalysts for the Fenton reaction have been studied, such as hematite, goethite, β-FeOOH [7–9]. However, many of these systems do not show favorable catalytic activity [10], which is particularly due to that Fe^{3+} cannot efficiently catalyze the generation of •OH from H_2O_2. At the same time, immobilized iron species on solid supports as promising heterogeneous catalysts have been developed recently. The supports can be organic and inorganic, natural and synthesized materials, such as zeolite [11], activated carbon [12], clay [13], silica [14], carbon aerogels [15], alginate gel beads [16], Nafion membrane [17], cationic exchange resin [18], etc. But these support catalyst face the obvious problems like iron leakage, instability in reuse or relatively low amount of iron loading and inconvenience in recycling. It also needs to be mentioned that organic supports could not stand durative attack of •OH and lack enough mechanic strength in general.

On the other hand, many researchers are focusing on applying some nonferrous metals with variable valence ions as Fenton-like catalysts. Luo et al. [19] prepared the $BiFeO_3$ magnetic nanoparticles as a catalyst to degrade Rhodamine B. The catalyst showed good catalytic performances. Han et al. [20] prepared the supported Au catalyst (Au/hydroxyapatite) which was proved to be effective in removing low level organic compounds. Cu-doped goethite and CuFeZSM-5 zeolite was prepared to oxidize organic substances in Fenton-like reaction by Guimaraes et al. [21] and Düankkci et al. [22], respectively. Han et al. [23] developed Mn_3O_4/SBA-15 catalyst for the complete oxidation of low concentration ethanol (100 ppm) by H_2O_2 in aqueous solution. Costa et al. [24] incorporated Co^{2+}, Mn^{2+} and Ni^{2+}, into the magnetite structure to increase the reactivity toward H_2O_2. Nonetheless, besides higher cost, the major problem confronting the use of the nonferrous metals is the toxicity which would lead to health problems because the poisonous metal leakage could not be completely avoided in use.

At present, endocrine disrupting compounds (EDCs) are introduced into the environment by anthropogenic discharge and now ubiquitous in aquatic environment [25–27]. However, it is still a very costly process to remove and degrade hydrophobic EDCs with too low concentration in vast drinking water source and environmental water even if take advantage of the effective Fenton

* Corresponding author. Tel.: +86 25 89680580; fax: +86 25 89680580.
E-mail addresses: xiaobinhu001@163.com (X.-b. Hu), envidean@nju.edu.cn (C. Sun).

0926-3373/$ – see front matter © 2012 Elsevier B.V. All rights reserved.
http://dx.doi.org/10.1016/j.apcatb.2012.08.018

method. To overcome the weakness of conventional Fenton reactions, a heterogeneous Fenton catalyst might be applicable with effective adsorption for hydrophobic EDCs, stable catalytic activity in reuse, and convenient recycle in water treatment.

The inverse spinel Fe_3O_4 has been investigated to have efficient catalysis in heterogeneous Fenton system because the Fe^{2+} in Fe_3O_4 plays an important role in the initiation of the Fenton reaction according to the classical Haber–Weiss mechanism [24]. Due to the hydrophobic surfaces, multiwalled carbon nanotubes (MWCNTs) are an effective adsorbent for hydrophobic organic chemicals in water treatment [28]. A novel catalyst, inverse-spinel ferroferric oxide nanoparticles decorated multiwalled carbon nanotubes (Fe_3O_4/MWCNTs) was successfully prepared and could applied for the adsorption and degradation of trace hydrophobic EDCs in the presence of H_2O_2. The novel catalyst has good structural stability, little iron leaching, stable catalytic activity in repetitive reaction cycle, and can be easily separated by outer magnet [29].

So far, many studies have been conducted to focus on the removal of EDCs from the environment [30,1,31,32]. However, the relationship of the fate and hormone activity of the EDCs during these processes was not explored in detail. It is important to know how efficiently they are removed by the Fenton oxidation and how the hormone activity changes during this process.

17α-Methyltestosterone (MT) is a well-known artificial androgen and has been widely used in aquaculture for seedling rearing and sex control and the treatment of male hypogonadism and delayed puberty [33–35]. This study focused on the investigation of the transformation mechanism and reduction of androgenic activity of MT from water by a novel Fe_3O_4/MWCNTs nanocomposites in a heterogeneous Fenton process. The intermediates were identified by GC–MS. Quantum calculations were also carried out to ascertain the position of the MT molecule at which the catalytic oxidation is initiated. On the basis of the results, a degradation mechanism was proposed in detail that would be useful to explain the loss of binding capacity of MT to androgen receptors. Human androgen ELISA test kits were used for the detection of androgenic activity of the degradation samples. The catalyst would be of potential application in eliminating hydrophobic compounds in water body.

2. Materials and methods

2.1. Chemicals

MT (>98.0%, the Laboratories of Dr. Ehrenstorfer Gmbh, Germany) was used without further purification. MWCNTs (>95%) with a mean outside diameter of 10–20 nm, were purchased from Alpha Nano Technology Co. Ltd. (Chengdu, China). The water employed was deionized. All the other chemicals used were of analytical grade and all the solvents used were of high-performance liquid chromatography (HPLC) grade. Stock solution was prepared by dissolving desired amount of MT into methanol in brown volumetric flask and stored in icebox at 4 °C. Working solutions were prepared by diluting stock solution with methanol to desired concentrations.

2.2. Heterogeneous Fenton recycling experiments

The heterogeneous catalyst Fe_3O_4/MWCNTs was prepared according to the previous work [29]. Briefly, the suspension containing 10 mg MWCNTs treated by the mixture of sulfuric acid/nitric acid was bubbled with N_2 flow to remove the dissolved oxygen and placed in a 95 °C water bath, then 2 g $FeSO_4{\cdot}7H_2O$ was added into the suspension. Afterwards, the solution containing 1.8 g NaOH and 0.9 g $NaNO_3$ was heated up to 95 °C and added into the heating suspension while kept vigorous stirring. The suspension kept heating at 95 °C for 2 h, the Fe_3O_4/MWCNTs nanocomposites formed. The MWCNTs content in the nanocomposites was about 1–2 wt%.

The chemical reactor was made of a 500 mL Pyrex beaker equipped with a mechanically stirrer. 1 mL MT methanol solution with desired concentration was added into the beaker. The methanol in the beaker was blown away by a mild N_2 flow to avoid the influence of methanol on the Fenton degradation for MT. 200 mL deionized water was then added into the beaker. The final MT water solution was acquired by placing the beaker in an ultrasound wave cleaner (40 kHz and 100 W) for 3 min. The pH of the reaction system was adjusted. The degradation experiment was subsequently started by adding required amount of Fe_3O_4/MWCNTs nanoparticles and H_2O_2 with mechanically stirring. For each oxidation reaction, the suspension solution was clarified quickly by an outer strong permanent magnet at the selected reaction time. The aqueous phase was sampled for analysis. The solid catalyst separated from aqueous phase was rinsed by 5 mL methanol for three times. The rinsed liquid was mixed for analysis. The residual MT amount is the sum of that in aqueous and solid phase. The recycling experiments were repeated seven times under the same experimental conditions. Heterogeneous catalyst samples also were analyzed by FTIR spectroscopy using a Necolet 5700 FTIR spectrometer (Thermo Electron Co.). The treated samples analyzed by HPLC (Agilent, USA 1200) [29]. Absorption spectrum scanning curves of clarified solutions of MT with and without the presence of HA and the catalyst were obtained by using a UV–vis spectrophotometer (754PC, Jinghua Instruments Inc., China).

2.3. Intermediates analyses

The degradation sample was concentrated by solid-phase extraction cartridge (C18-M, Phenomenex, USA) and eluted with 1:1 (v:v) acetone/methanol followed by N_2 gas bubbling. Chemical analysis of intermediates of MT Fenton degradation was carried out using a GC–MS system (Agilent 6890/5975, USA) equipped with a fused silica capillary column (DB-5MS, 30 m long, 0.25 mm i.d., 0.25 μm film thickness). A split–splitless injection port was used in the splitless mode at high pressure (19.2 kPa). The column temperature was programmed as follows: 2 min at 50 °C, 20 °C min^{-1} to 200 °C, 5 °C min^{-1} to 300 °C, and 30 min at 300 °C. The helium gas flow rate was 1.63 mL min^{-1} (at 50 °C). Electron impact was used for ionization of samples. Some of the intermediates were identified by an identification program of the U.S. National Institute of Standards and Technology (NIST) library.

2.4. Calculation of the Frontier electron density and bond dissociation enthalpies (BDEs)

The ab initio molecular orbital (MO) calculations were carried out by using Gaussian 03 program (Gaussian, Inc.). Structures were fully optimized with the b3lyp/6-31G* basis set at the level of the Density Functional Theory (DFT) for all calculations, and then the Frontier electron densities (FEDs) of the highest occupied molecular orbital (HOMO) and the lowest unoccupied molecular orbital (LUMO) were calculated. The values of ($FED_{HOMO}{}^2 + FED_{LUMO}{}^2$) were obtained to predict the reaction sites for radical attack [36]. The C—H bond dissociation enthalpies (BDEs) and O—H BDEs of MT were also calculated to predict the reaction sites for abstracting hydrogen reaction initiated by hydroxyl radical [37,38].

2.5. Evaluation of androgenic activities for treated water

Double antibody sandwich ELISA test kits (Human androgen ELISA, Shanghai Jingma Biotechnology Co. Ltd.) were used for the detection of androgenic activity of the degradation samples

in the study. A Lab-tech HTIII Microplate Reader (Anthos Labtec Instruments GmbH, Austria) was used to read the absorbance on ELISA plates at 450 nm.

3. Results and discussion

3.1. Performance of MT Degradation by nano Fe_3O_4/MWCNTs Fenton process

The novel catalyst, inverse-spinel ferroferric oxide nanoparticles decorated MWCNTs was prepared by the regular growth of ferroferric oxide crystal from the Fe^{2+} adsorbed on modified MWCNTs in hot alkaline and oxidizing solution [29]. Magnetism makes Fe_3O_4/MWCNTs be very easily separated from the reaction medium by an external magnetic field. The morphology of Fe_3O_4/MWCNTs showed the octahedron Fe_3O_4 nanoparticles growing on the MWCNTs surface regularly with diameters ranging from 40 to 100 nm and most of the Fe_3O_4 nanoparticles were strung by MWCNTs [29]. The Fe_3O_4/MWNTs nanocomposites exhibited much higher adsorption capacity for MT than bare Fe_3O_4 under the reaction conditions ([MT] = 0.212 mg L^{-1}, [Fe_3O_4/MWCNTs] = 2 g L^{-1}, H_2O_2 = 5 mM, T = 20°C, pH 5). The solution pH is also an important factor that dramatically influences the efficiency of the Fenton reaction. In the previous work, we reported that the degradation process remained efficient and feasible from pH 2.5 to 5.0 [29].

An attractive catalyst, besides its high catalytic capacity, and easy separation, must exhibit a superior stable catalytic ability for repeated uses. After seven catalytic cycles of 8 h of degradation, the average degradation efficiency of MT was 82.7% and an average iron leaching concentration of 0.59 mg L^{-1}, which showed almost no difference with the first oxidation cycle under the identical reaction conditions. Besides, the XRD of the used Fe_3O_4/MWCNTs and the TEM image was found to be the same as that recorded before reaction [29]. Fig. S1 showed the magnetization hysteresis loops of the fresh and used Fe_3O_4/MWCNTs sample. It could be seen that the saturation magnetization of the fresh and used sample were 79.4 emu g^{-1} and 76.3 emu g^{-1}, respectively, which were very close but lower than the value of the corresponding pure bulk ferrites (Fe_3O_4, 93 emu g^{-1}) and it may be most likely due to the nanometer size of Fe_3O_4 and the existence of MWCNTs [39]. The FTIR spectra of Fe_3O_4/MWCNTs samples were shown in Fig. S2. A very strong IR band at 3396 cm^{-1} could be ascribed to the O—H stretching vibration of surface H_2O molecules and OH groups of modified MWCNTs. A strong peak at 572 cm^{-1} may correspond to the stretching vibration of Fe—O—Fe in Fe_3O_4 [40]. After seven catalytic cycles of Fe_3O_4/MWCNTs, the FTIR spectrum of Fe_3O_4/MWCNTs was the same as the original catalyst. Results showed that the catalytic center of Fe_3O_4/MWCNTs did not inactivate or changed its chemical constituents obviously. Duarte et al. [15] reported that in the first trial, the decomposition degree of Orange II by Fe/carbon aerogels was 95%, while in the third trial, the decomposition degree was 80%. And the degradation half-lives delayed three times from the 1st to the 3rd cycle. Ramirez et al. [41] also found that the degradation of Orange II on the reused Fe/carbon catalyst was significantly decreased. As compared with the Fe/carbon, Fe_3O_4/MWCNTs showed a better stability for reuse.

3.2. Mass transfer rate and chemical reaction rate

In heterogeneous catalytic system, the reaction process usually included two successive steps, the diffusion of the reactants to the surface of the catalysts and subsequently the transformation of the reactants into intermediates or products. Thus the apparent rate of a heterogeneous reaction is usually controlled by either the rate of diffusion of the solutes to the surface or the rate of intrinsic chemical reactions on the surface. In order to elucidate the rate-controlling step, the reaction-diffusion modulus (Thiele modulus, φ) was estimated [42]. φ is expressed as the ratio of the reaction rate to the diffusion rate

$$\varphi = \left[\frac{k}{D/L^2}\right]^{0.5}$$

where k is the first-order reaction rate constant (s^{-1}), D is the diffusion coefficient ($cm^2\ s^{-1}$), and L is the thickness of the stagnant liquid film (cm). If φ is estimated to be >5, the diffusion of reactant from the bulk of the solution to the surface is the controlling step, but φ < 0.5 suggests a slow reaction rate.

The MT degradation and H_2O_2 decomposition approximately followed a pseudo-first-order reaction in kinetics under tested conditions, which may be expressed as $\ln(c_t/c_0) = kt + A$, where A is a constant, t is reaction time (s), k is the pseudo-first-order rate constant (s^{-1}), and c_0 and c_t are MT or H_2O_2 concentrations (mmol L^{-1}) at time of t = 0 and t = t, respectively. The k measured for the MT oxidation rate and for the decomposition of H_2O_2 was $1.1 \times 10^{-4}\ s^{-1}$ (r^2 = 0.942) (Fig. 1) and $3.2 \times 10^{-5}\ s^{-1}$ (r^2 = 0.985) (Fig. 2), respectively. Maybe owing to the enrichment of the MT onto the surface of the catalyst, the degradation rate of MT at initial stage was much faster than later stage. Thus the degradation intermediates and products might run up on the surface of the catalyst or in

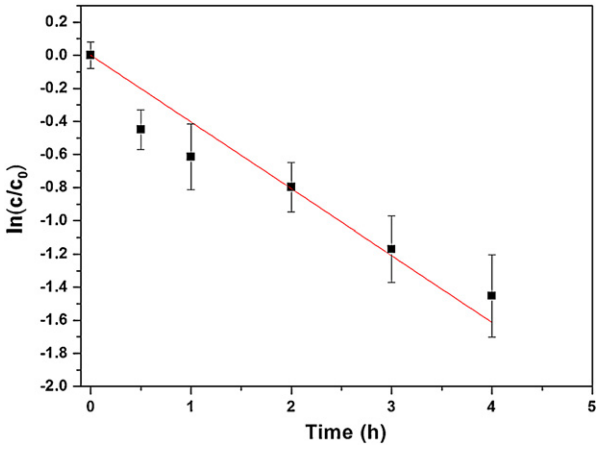

Fig. 1. Pseudo-first-order fitting of MT degradation kinetic data ([Fe_3O_4/MWCNTs] = 2 g L^{-1}, [H_2O_2]$_0$ = 5.3 mmol L^{-1}, [MT]$_0$ = 212 μg L^{-1}, pH 5, T = 20 °C).

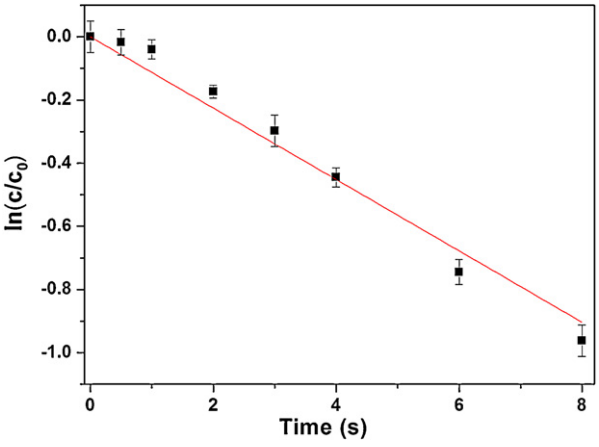

Fig. 2. Pseudo-first-order fitting of H_2O_2 decomposition kinetic data ([Fe_3O_4/MWCNTs] = 2 g L^{-1}, [H_2O_2]$_0$ = 5.3 mmol L^{-1}, [MT]$_0$ = 212 μg L^{-1}, pH 5, T = 20 °C).

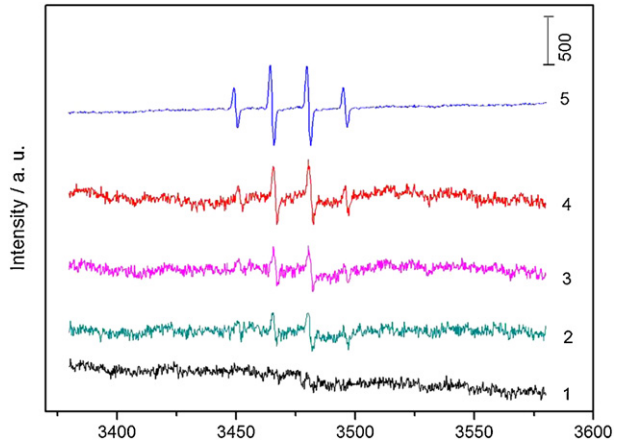

Fig. 3. DMPO spin-trapping ESR spectra of •OH in the system of (1) MWCNTs–H_2O_2–MT, pH 5; (2) reused Fe_3O_4/MWCNTs–H_2O_2–MT, pH 5; (3) Fe_3O_4/MWCNTs–H_2O_2–MT, pH 5; (4) Fe_3O_4/MWCNTs–H_2O_2–MT, pH 4 and (5) Fe_3O_4–H_2O_2–MT, pH 4. [Fe_3O_4/MWCNTs] or [Fe_3O_4] = 2 g L^{-1}, [H_2O_2]$_0$ = 5.3 mmol L^{-1}, [MT]$_0$ = 212 μg L^{-1}.

the reaction system, which caused an obvious slowing down of the degradation rate of MT in subsequently phase. This resulted in a deviation from the pseudo-first order reaction. The diffusion coefficient of the solutes in liquids is typically ~10^{-5} cm^2 s^{-1}, and the maximum value of the stagnant layer thickness of the liquid film was hypothesized as ~0.5×10^{-5} cm considering the diameter range of the particles when the catalyst was completely dispersed. So the estimated φ was 1.66×10^{-5} for the MT oxidation and 0.89×10^{-5} for the decomposition of H_2O_2, respectively. The value of φ implied that the average rate of the reaction of MT and H_2O_2 on the catalyst surface was far slower than its diffusion rate to the surface through the external film. Therefore, the intrinsic reactions on the oxide surface including sorption and oxidation are expected to be the rate-limiting steps for this process.

3.3. Competitive oxidation

The generation of •OH was monitored by ESR (Fig. 3). The ESR spectrum in the presence of Fe_3O_4/MWCNTs and Fe_3O_4 displayed a 4-fold characteristic peak of the typical DMPO-•OH adduct with an intensity ratio of 1:2:2:1. The intensity of the signal increased with the decrease of the system pH. This phenomenon was in agreement with the results of the degradation experiment of MT (Fig. 4). However, no ESR signal of DMPO-•OH adduct was found

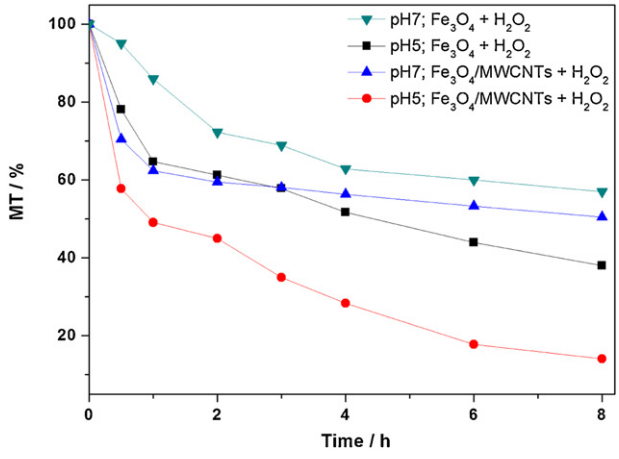

Fig. 4. The MT degradation in water under different conditions ([Fe_3O_4/MWCNTs] or [Fe_3O_4] = 2 g L^{-1}, [H_2O_2] = 5.3 mmol L^{-1}, [MT] = 212 μg L^{-1}, T = 20 °C).

in the presence of the modified MWCNTs, which implied that the MWCNTs–H_2O_2 system could not produce detectable •OH. The intensity in the Fe_3O_4–H_2O_2 system was obviously higher than that in the Fe_3O_4/MWCNTs–H_2O_2 system. Usually, due to the delocalized π-bond, the remain fraction (free radical) of the aromatic phenol-like structure is relatively stable after the hydrogen of the phenol hydroxyl group was abstracted by •OH, which makes aromatic phenol-like structure with hydroxyl function to be an effective •OH scavenger. We supposed that there were a number of hydroxyl functions existing in the defect sites on the surface of the modified MWCNTs oxidized by mixed acids, which resulted in the formation of some structures similar to the aromatic phenol which were scavengers of •OH. But the oxidation rate of MT in the Fe_3O_4/MWCNTs–H_2O_2 system was obtained to be higher than that in the Fe_3O_4–H_2O_2 system. These results implied that besides the concentration of •OH, an important reason as discussed below probably affected the degradation rate in the two reaction systems.

Lin and Gurol [42] listed the rate constants of H_2O_2 reacting with •OH, HO_2•, Fe^{2+}/$FeOH^+$, and Fe^{3+} in the $Fe^{III}(Fe^{II})$–H_2O_2 system. The rate constant of H_2O_2 reacting with •OH is much higher at least five orders of magnitude than that of other reactions. So it was suggested that H_2O_2 was one of the main removers of •OH.

In fact, there were competition oxidation between •OH and two probable main reactants in the aqueous system studied, MT and H_2O_2.

$$\text{•OH} + \text{MT} \rightarrow \text{products} \quad (1)$$

$$\text{•OH} + H_2O_2 \rightarrow \text{products} \quad (2)$$

The reaction rate could be expressed as follows:

$$\frac{-\mathrm{d}[\mathrm{MT}]}{\mathrm{d}t} = k_1[\mathrm{MT}][\text{•OH}] \quad (3)$$

$$\frac{-\mathrm{d}[H_2O_2]}{\mathrm{d}t} = k_2[H_2O_2][\text{•OH}] \quad (4)$$

where k_1 and k_2 were the rate constants. Here, it was assumed that in the degradation process, the [•OH] was at steady state. The reactions (1) and (2) approximately followed the pseudo-first-order reaction in kinetics.

$$\frac{-\mathrm{d}[\mathrm{MT}]}{\mathrm{d}t} = k_1'[\mathrm{MT}] \quad (k_1[\text{•}OH] = k_1') \quad (5)$$

$$\frac{-\mathrm{d}[H_2O_2]}{\mathrm{d}t} = k_2'[H_2O_2] \quad (k_2[\text{•OH}] = k_2') \quad (6)$$

The relative rate of the two competitive reaction could be expressed as follows [43]:

$$\frac{\mathrm{d}[H_2O_2]/\mathrm{d}t}{\mathrm{d}[\mathrm{MT}]/\mathrm{d}t} = \frac{k_2[H_2O_2][\text{•OH}]}{k_1[\mathrm{MT}][\text{•OH}]} = \frac{k_2[H_2O_2]}{k_1[\mathrm{MT}]} \approx 2422 \quad (7)$$

The relative rate of reaction could be simply estimated (i.e., 2422). With relatively very high concentrations of H_2O_2 (0.18 g L^{-1}; 5.3 m mol L^{-1}) in the reaction system relative to MT (212 μg L^{-1}; 7.0×10^{-4} m mol L^{-1}), •OH reacts more rapidly with H_2O_2 than with MT, which implied that H_2O_2 was a more important •OH scavenger than MT in the reaction system.

It can be observed from Fig. 4 that the Fe_3O_4/MWCNTs showed a higher catalytic capability than the bare Fe_3O_4 for the degradation of MT in the presence of H_2O_2, especially during the initial phase of the degradation reactions. In the Fe_3O_4/MWCNTs–H_2O_2 system, the conversion rates of MT after 8 h reaction were 85.9% (pH 5) and 50.5% (pH 7), respectively. However, the conversion rates were 62.0% (pH 5) and 43.0% (pH 7) in the Fe_3O_4–H_2O_2 system, respectively. In the previous work, results showed that the synthesized Fe_3O_4/MWCNTs had much higher ability for the adsorption of trace MT than Fe_3O_4 in aqueous solution, and the sorption–desorption processes were fast dynamic equilibrium process compared with

Table 1
Intermediates of MT degradation detected by GC–MS.

Peak	t_R (min)	EI-MS spectrum ions (m/z) (relative abundance, %)	Possible structure
a	18.937	290 (3.5); 272 (24); 257 (16); 233.2 (62); 215 (52); 201 (22); 176 (20); 161 (24); 145 (43); 121 (30); 97 (100); 79 (47);	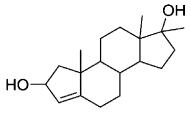
b	19.313	284 (40); 269 (100); 251 (8.8); 225 (6.6); 211 (3.5); 195 (4.0); 173 (11); 161 (21); 145 (41); 105 (30); 91 (40); 79 (20)	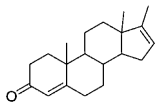
c	20.422	288 (51); 273 (35); 250 (23); 231 (16); 213 (39); 199 (24); 174 (32); 161 (56); 145 (29); 123 (86); 105 (63); 91 (68)	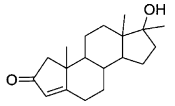
d	21.041	300 (89); 285 (10); 267 (13); 245 (51); 229 (47); 215 (8.1); 202 (14); 178 (30); 148 (59); 121 (63); 107 (64); 91 (100)	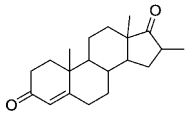
e	21.695	318 (8.2), 300 (20); 275 (16); 261 (20); 243 (17); 187 (27); 163 (45); 147 (32); 125 (86); 109 (60); 95 (56); 79 (64); 43 (100)	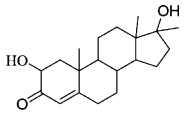
f	22.264	318 (1.5); 302 (58); 284 (28); 269 (41); 229 (100); 213 (61); 173 (38); 159 (46); 119 (59); 105 (86); 91 (93); 43 (94)	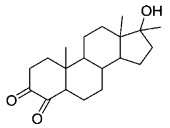
g	23.657	302 (100); 284 (15); 245 (28); 229 (34); 202 (27); 187 (20); 161 (34); 149 (29); 124 (92); 105 (47); 91 (62); 43 (90)	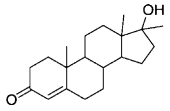
h	23.941	316 (5.1); 300 (57); 282 (60); 267 (98); 242 (54); 227 (30); 185 (25); 173 (35); 159 (50); 136 (79); 91 (80); 43 (100)	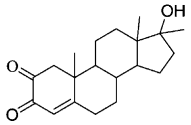
i	24.019	300 (1.0); 282 (3.6); 242 (7.0); 179 (5.0); 161 (20); 147 (20); 134 (16); 122 (100); 108 (18); 91 (27); 77 (11); 55 (6.0); 43 (25)	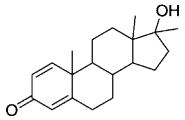
j	26.621	318 (6.0); 300 (12); 282 (38); 242 (32); 232 (44); 217 (16); 159 (25); 137 (28); 124 (58); 105 (48); 87 (78); 43 (100)	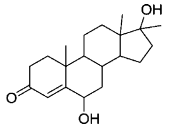

the timescale of the chemical degradation reaction. The heterogeneous reaction was the dominant way for the degradation of MT in the Fe_3O_4/MWCNTs–H_2O_2 system [29]. In the preparation of the catalyst, owing to the electrostatic adsorption, the iron ions occupied the functionalized sites (broken surface) of the treated MWCNTs where the Fe_3O_4 nano particles formed by in situ growth. The MT in the degradation solution was inclined to be absorbed onto the hydrophobic surface of the MWCNTs (unbroken surface) for its strong hydrophobicity. It was supposed that •OH would be consumed in the very near vicinity of or on the catalyst surface prior to diffusing to the solution. Thus the enriched MT in the very near vicinity of the catalyst surface may lead to a more efficient •OH scavenging action when competed with H_2O_2. It can be seen from Fig. 5 that just 63.5% MT transformed when 2.5 mg L^{-1} humic acid (HA) was added into the system. The conversion rate showed an obvious decrease when compared with the aforementioned results in Fe_3O_4/MWCNTs-system without HA. The competitive reaction might also explain the decrease of MT degradation rate in the reaction system spiked with HA which could be adsorbed onto the catalyst surface and consume •OH. As shown in Fig. 6, a remarkable decrease of the absorbance of HA in the clarified water solution implied that most of the HA was adsorbed by the catalyst. It can be deduced from the changes of the strength of the absorption peak that Fe_3O_4 showed poor adsorption ability of MT but great adsorption ability for HA.

3.4. Possible degradation mechanism of MT

The Fenton oxidation of organic compounds will bring about many intermediates. To elucidate the structures of the intermediates, the degradation sample was extracted and concentrated and then detected by GC–MS equipped with an identification program

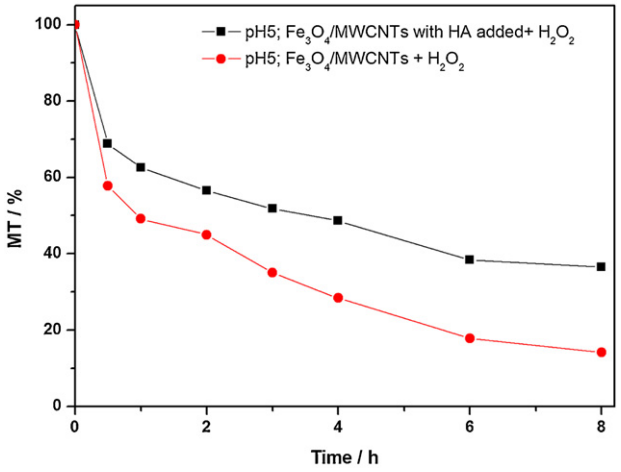

Fig. 5. The MT degradation in water with or without HA added ([Fe_3O_4/MWCNTs] = 2 g L^{-1}, [H_2O_2] = 5.3 mmol L^{-1}, [MT] = 212 μg L^{-1}, T = 20 °C).

obtained from NIST. The GC–MS chromatogram was shown in Fig. S3. GC–MS results (Table 1) obtained in the present study indicated the peaks of 17α-methyltestosterone (RT 23.657 min) and methandrostenolone (RT 24.019 min) with similarities of 99 and 93%, respectively. Most peaks of intermediates were not identified clearly in the GC–MS analysis because the mass spectra look similar to each other and there are no spectra of the unknown intermediates in the database. Because of the deficiency of the standard substances, it was attempted to elucidate the degradation mechanism of MT by mass spectra analysis and molecular theory calculation.

Ohko et al. [36] studied the degradation of E2 in water by TiO_2 photocatalysis and calculated the FED of E2. They found the sites for the first addition by photocatalytically generated •OH could be predicted by the values of $FED_{HOMO}{}^2 + FED_{LUMO}{}^2$. A higher value of $FED_{HOMO}{}^2 + FED_{LUMO}{}^2$ implies a higher attack possibility of •OH. On the other hand, an important pathway of •OH scavenging by many organic compounds is hydrogen abstraction reaction [44]. A lower BDE value suggests a higher hydrogen abstraction possibility. To elucidate the sites for possible hydrogen abstraction reaction, the C—H BDEs and O—H BDEs of MT were also calculated. The calculated $FED_{HOMO}{}^2 + FED_{LUMO}{}^2$ on atoms and O—H and C—H BDEs of MT were listed in Table 2. According to Table 2, the intermediates produced in the subsequent reactions were shown

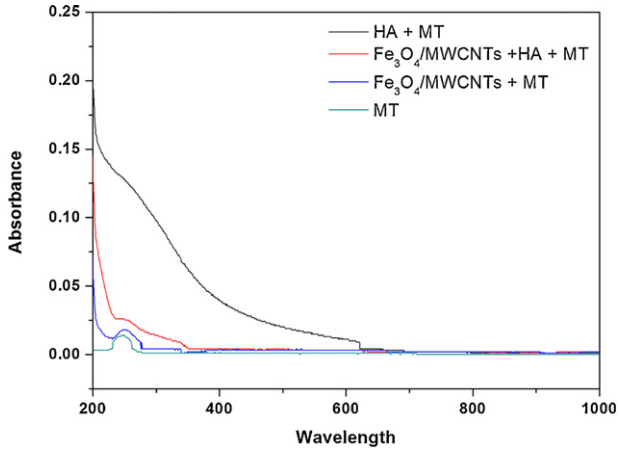

Fig. 6. Absorption spectrum scanning curves of clarified solutions of MT with and without the presence of HA and the catalyst ([Fe_3O_4/MWCNTs] = 2 g L^{-1}, [HA] = 2.5 mg L^{-1}, [MT] = 212 μg L^{-1}, T = 20 °C).

Table 2
Frontier electron densities (FED) and O—H BDE and C—H BDEs on atoms of MT calculated by using Guassian 03 Program with the b3lyp/6-31G* basis set at the level of the Density Functional Theory (DFT).

Atom	$FED_{HOMO}{}^2 + FED_{LUMO}{}^2$	Corresponding O—H BDE and C—H BDEs (kJ/mol)
C1	0.042	401.6
C2	0.161	370.1
C3	0.223	–
C4	0.248	458.8
C5	0.338	–
C6	0.027	329.2
C7	0.043	405.9
C8	0.027	393.3
C9	0.019	387.2
C10	0.018	–
C11	0.016	394.8
C12	0.002	402.9
C13	0.000	–
C14	0.001	371.3
C15	0.001	398.0
C16	0.000	395.6
C17	0.000	–
C18	0.000	412.6
C19	0.044	414.1
C20	0.000	414.9
O3	0.681	–
O17	0.000	391.9

in Scheme 1. The values of $FED_{HOMO}{}^2 + FED_{LUMO}{}^2$ were found to be high at the enone conjugated double bond moiety, especially at the O3 and C5 atoms. If the first addition of •OH occurred at the C5 atom, the corresponding intermediate 5 could be produced by a dehydration reaction after another •OH addition, as shown in Scheme 1 (MT → 3 → 4 → 5). However, if the first addition of •OH occurred at the O3 atom, MT probably could not be transformed after the elimination of a peroxide molecule at the C3 atom following another •OH attack (MT → 1 → 2 → MT). According to the BDEs, hydrogen abstraction reaction would occur at the C6 atom, intermediate 7 could be produced by another •OH addition to the radical (6) formed by hydrogen abstraction reaction (MT → 6 → 7). The hydrogen abstraction reaction at C2 atom led to the formation of methandrostenolone (10) after a dehydration reaction following another •OH addition (MT → 8 → 9 → 10). Since the double bond between C1 and C2 of methandrostenolone molecular could be attacked by •OH, intermediate 13 could be produced after a dehydration reaction following •OH addition (10 → 11 → 12 → 13). It is reasonable to consider that the interaction between these intermediates and the human androgen receptor should be changed. Because of conversion of the conjugated double bond structure of MT or increasing hydrophilicity by hydroxyl partly substituted MT, the intermediates should exhibit a much weaker androgenic activity than that of MT [45].

3.5. Elimination of androgenic activity of MT

It was found that many byproducts were formed in the heterogeneous Fenton degradation of MT. The removal rate and reduction of androgenic activity of MT in deionized water and drinking water matrices including Ca^{2+} (16.95 mg L^{-1}), Cl^- (14.33 mg L^{-1}), $NO_3{}^-$ (4.62 mg L^{-1}), F^- (0.46 mg L^{-1}), K^+ (6.45 mg L^{-1}), Na^+ (25.08 mg L^{-1}), $SO_4{}^{2-}$ (45 mg L^{-1}) and HA (2.5 mg L^{-1}) were quantitatively evaluated in response to androgen antibody by human androgen ELISA KIT (Fig. 7). In deionized water (pH was adjusted to 4.5), the androgenic activity of MT decreased from 93,014 to 24,377 IU L^{-1} with the MT concentration decreasing from 212 to 3.1 μg L^{-1} after 8 h of degradation in Fe_3O_4/MWCNTs–H_2O_2 system. When pH was adjusted to 3.5, the androgenic activity of the degradation sample decreased from 94,604 to 18,831 IU L^{-1} with

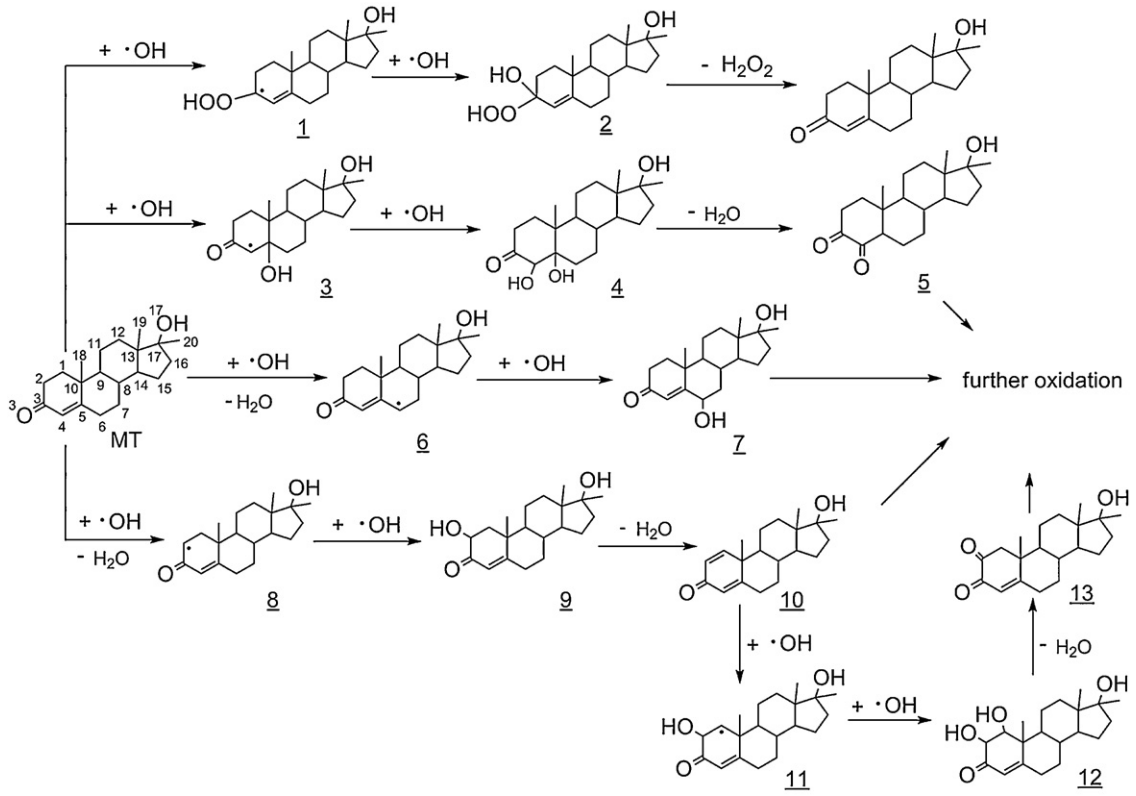

Scheme 1. Possible mechanism of MT Fenton degradation.

the MT concentration decreasing from 212 to 1.1 μg L^{-1} after 8 h. The binding affinity of MT degradation samples with androgenic antibody decreased with reaction time. The trend in the drinking water system was similar to that of the MT androgenic activity in distilled water. But the decrease rates of the androgenic activity and MT concentration in drinking water obviously slowed down, respectively, compared with those in distilled water. The sample activity decreased from 93,014 to 40,089 IU L^{-1} with MT concentration decreasing from 212 to 41.29 μg L^{-1} after 8 h.

Studies have shown that the ketone group at the third carbon atom in MT molecule is the active site that can bind with specific receptor and makes the molecule have androgenic activity

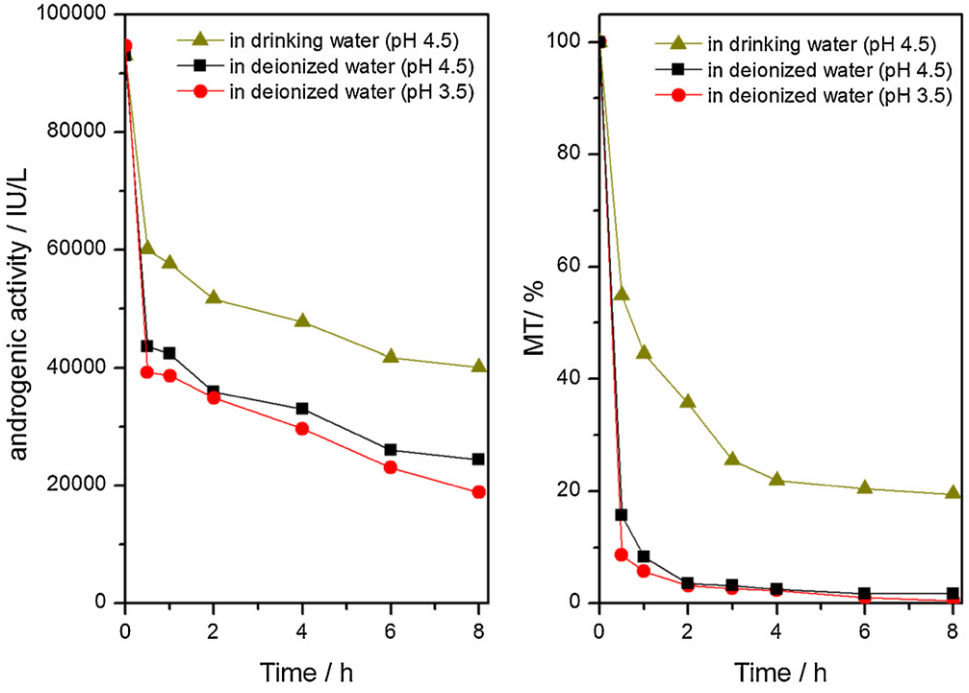

Fig. 7. Reduction of concentration and androgen activity of MT during the Fenton process ([Fe_3O_4/MWCNTs] = 2 g L^{-1}, [H_2O_2] = 5.3 mmol L^{-1}, [MT] = 212 μg L^{-1}, T = 20 °C).

[45]. The calculation based on quantum chemistry showed that the ketone group in the structure of conjugated double bond in MT molecule was easy to be attacked by •OH. Androgenic activity has strict structure specificity. Even a little modification of testosterone molecule will make its androgenic activity decrease including demethylation and displacement reaction at A ring or fused rings. It is likely that the Fenton reaction may quickly decrease the capacity of MT to bind to the androgenic receptor. It can be seen from Fig. 7 that there was no significant difference between the changing trends of oxidation and reduction of androgenic activity for MT treated in Fe_3O_4/MWCNTs–H_2O_2 system. Therefore, it can be deduced that the observed degradation in the parent compound corresponds directly to the reduction in androgenic activity. The similarity between MT removal rate and androgenic activity removal rate implied that none of the oxidation byproducts produced in the reaction is comparable to the parent compound in terms of androgenic activity. However, the results also showed that the androgenic activity of the intermediates cannot be removed completely in 8 h degradation time. Ohko et al. [36] and Zhao et al. [7] previously reported that the estrogenic activity of E2 should almost be lost concurrently with the decrease of E2 concentration in photocatalytic reaction system. Likewise, as a steroid like MT, E2 could be degraded by photo-Fenton reaction via oxidation of the active site (phenol moiety), which is known to be critical for receptor binding and conferral of estrogenicity to steroid estrogens.

4. Conclusions

A novel heterogeneous Fenton catalyst, Fe_3O_4/MWCNTs was evaluated through the degradation of MT in the presence of H_2O_2. The intrinsic reactions on the oxide surface were the rate-limiting steps for the degradation process. There is a competition in the reaction of •OH with MT and H_2O_2. The enrichment of trace MT on the catalyst surface by the adsorption might favor the competition oxidation of MT. The spiked HA could be adsorbed onto the catalyst surface and consume •OH, which led to the decrease of MT degradation rate in the reaction system. GC–MS and theoretical calculation of frontier electron densities and bond dissociation enthalpies were used to identify the oxidation intermediates and help to gain a deeper insight of the reaction mechanism. The ketone group in the structure of conjugated double bond in MT molecule was easy to be attacked by •OH. The Fenton oxidation may quickly decrease the capacity of MT to bind to the androgenic receptor. There was no significant difference between the changing trends of oxidation and reduction of androgenic activity for MT treated in Fe_3O_4/MWCNTs–H_2O_2 system.

Acknowledgements

The present research supported by the National Natural Science Major Foundation of China (no. 5093800) and National Natural Science Foundation of China (no. 21177055)

Appendix A. Supplementary data

Supplementary data associated with this article can be found, in the online version, at http://dx.doi.org/10.1016/j.apcatb.2012.08.018.

References

[1] S.M. Arnold, W.J. Hickey, R.F. Harris, Environmental Science and Technology 29 (1995) 2083–2089.
[2] E. Neyens, J. Baeyens, Journal of Hazardous Materials 98 (2003) 33–50.
[3] A. Georgi, F.D. Kopinke, Applied Catalysis B: Environmental 58 (2005) 9–18.
[4] I.A. Salem, Applied Catalysis B: Environmental 28 (2000) 153–162.
[5] M. Perez, F. Torrades, X. Domenech, J. Peral, Water Research 36 (2002) 2703–2710.
[6] M. Neamtu, C. Catrineseu, A. Kettrup, Applied Catalysis B: Environmental 51 (2004) 149–157.
[7] Y.P. Zhao, H.Y. Hu, Applied Catalysis B: Environmental 78 (2008) 250–258.
[8] S.S. Chou, C.P. Huang, Chemosphere 38 (1999) 2719–2731.
[9] J.Y. Feng, X.J. Hu, P.L. Yue, H.Y. Zhu, G.Q. Lu, Water Research 37 (2003) 3776–3784.
[10] W.P. Kwan, B.M. Voelker, Environmental Science and Technology 37 (2003) 1150–1158.
[11] E.V. Kuznetsova, E.N. Savinov, L.A. Vostrikova, V.N. Parmon, Applied Catalysis B: Environmental 51 (2004) 165–170.
[12] A. Dhaouadi, N. Adhoum, Applied Catalysis B: Environmental 97 (2010) 227–235.
[13] L.F. Liotta, M. Gruttadauria, G.D. Carlo, G. Perrini, V. Librandod, Journal of Hazardous Materials 162 (2009) 588–606.
[14] L. Hacgyu, L. Jinwoo, J. Sunmi, K. Jaeyun, Y. Jeyong, H. Taeghwan, Chemical Communications 28 (2006) 463–465.
[15] F. Duarte, F.J. Maldonado-Hódar, A.F. Pérez-Cadenas, L.M. Madeira, Applied Catalysis B: Environmental 85 (2009) 139–147.
[16] J. Fernandez, M.R. Dhananjeyan, J. Kiwi, Y. Senuma, J. Hilborn, Journal of Physical Chemistry B 104 (2000) 5298–5301.
[17] P. Maletzky, R. Bauer, J. Lahnsteiner, B. Pouresmael, Chemosphere 38 (1999) 2315–2325.
[18] M.M. Cheng, W.H. Ma, J. Li, Y.P. Huang, J.C. Zhao, Environmental Science and Technology 38 (2004) 1569–1575.
[19] W. Luo, L.H. Zhu, N. Wang, H.Q. Tang, M.J. Cao, Y.B. She, Environmental Science and Technology 44 (2010) 1786–1791.
[20] Y.F. Han, N. Phonthammachai, K. Ramesh, Z.Y. Zhong, T. White, Environmental Science and Technology 42 (2008) 908–912.
[21] I.R. Guimaraes, A. Giroto, L.C.A. Oliveira, M.C. Guerreiro, D.Q. Lima, J.D. Fabris, Applied Catalysis B: Environmental 91 (2009) 581–586.
[22] M. Düankkci, G. Gündüz, S. Yılmazb, R.V. Prihod'koc, Journal of Hazardous Materials 181 (2010) 343–350.
[23] Y.F. Han, F.X. Chen, K. Ramesh, Z.Y. Zhong, E. Widjaja, L.W. Chen, Applied Catalysis B: Environmental 76 (2007) 227–234.
[24] R.C.C. Costa, M.F.F. Lelis, L.C.A. Oliveira, J.D. Fabris, J.D. Ardisson, R.R.V.A. Rios, C.N. Silva, R.M. Lago, Journal of Hazardous Materials B129 (2006) 171–178.
[25] C. Sonnenschein, A.M. Soto, Journal of Steroid Biochemistry and Molecular Biology 65 (1998) 143–150.
[26] A.C. Belfroid, A. Van der Horst, A.D. Vethaak, A.J. Schafer, G.B.J. Rijs, J. Wegener, W.P. Cofino, Science of the Total Environment 225 (1999) 101–108.
[27] G.R. Boyd, H. Reemtsma, D.A. Grimm, S. Mitra, Science of the Total Environment 311 (2003) 135–149.
[28] B. Pan, B.S. Xing, Environmental Science and Technology 42 (2008) 9005–9013.
[29] X.B. Hu, B.Z. Liu, Y.H. Deng, H.Z. Cheng, S. Luo, C. Sun, P. Yang, S.G. Yang, Applied Catalysis B: Environmental 107 (2011) 274–283.
[30] R.A. Torres, C. Pétrier, E. Combet, F. Moulet, C. Pulgarin, Environmental Science and Technology 41 (2007) 297–302.
[31] J. Herney-Ramirez, M.A. Vicente, L.M. Madeira, Applied Catalysis B: Environmental 98 (2010) 10–26.
[32] H. Katsumata, S. Kawabe, S. Kaneco, T. Suzuki, K. Ohta, Y. Yobiko, Chemosphere 63 (2006) 592–599.
[33] R.L. Sharpe, D.L. MacLatchy, S.C. Courtenay, G.J. Vanderkrak, Aquatic Toxicology 67 (2004) 203–215.
[34] L. Andersen, R. Goto-Kazeto, J.M. Trant, J.P. Nash, B. Korsgaard, P. Bjerregaard, Aquatic Toxicology 76 (2006) 343–352.
[35] M. Seki, H. Yokota, H. Matsubara, M. Maeda, H. Tadokoro, K. Kobayashi, Environmental Toxicology and Chemistry 23 (2004) 774–781.
[36] Y. Ohko, K.I. Iuchi, C. Niwa, T. Tatsuma, T. Nakashima, T. Iguchi, Y. Kubota, A. Fujishima, Environmental Science and Technology 36 (2002) 4175–4181.
[37] M. Kılıç, G. Koçtürk, N. San, Z. Çınar, Chemosphere 69 (2007) 1396–1408.
[38] L.F. Wang, H.Y. Zhang, Bioorganic and Medicinal Chemistry Letters 13 (2003) 3789–3792.
[39] B.P. Jia, L. Gao, J. Sun, Carbon 45 (2007) 1476–1481.
[40] A.K. Mishra, S. Ramaprabhu, Journal of Physical Chemistry C 114 (2010) 2583–2590.
[41] J.H. Ramirez, F.J. Maldonado-Hódar, A.F. Pérez-Cadenas, C. Moreno-Castilla, C.A. Costa, L.M. Madeira, Applied Catalysis B: Environmental 75 (2007) 312–323.
[42] S.S. Lin, M.D. Gurol, Environmental Science and Technology 32 (1998) 1417–1423.
[43] S.G. Huling, P.K. Jones, T.R. Lee, Environmental Science and Technology 41 (2007) 4090–4096.
[44] Y.P. Qian, Y.J. Shang, Q.F. Teng, J. Chang, G.J. Fan, X. Wei, R.R. Li, H.P. Li, X.J. Yao, F. Dai, B. Zhou, Food Chemistry 126 (2010) 241–248.
[45] A.G. Fragkaki, Y.S. Angelis, M. Koupparis, A. Tsantili-Kakoulidou, G. Kokotos, C. Georgakopoulos, Steroids 74 (2009) 172–197.